Supporting Information for

Omnidirectionally Stretchable Electrodes Based on Wrinkled Silver Nanowires Through the Shrinkage of Electrospun Polymer Fibers

Chen Ding, [a#] Qingsong Li, [b#] Yong Lin, [a] Xinzhou Wu, [a] Zeyu Wang, [c] Wei Yuan, [a*] Wenming Su, [a] Wei Chen, [c] and Zheng Cui [a*]

[a] Printable Electronics Research Centre, Suzhou Institute of Nano-Tech and Nano-Bionics, Chinese Academy of Sciences, Suzhou 215123, China.

[b] CAS Key Laboratory of Human-Machine Intelligence-Synergy Systems, Shenzhen Institutes of Advanced Technology, Chinese Academy of Sciences (CAS), Shenzhen, 518055 China.

[c] Center for Intelligent Medical Electronics, School of Information Science and Engineering, Fudan University, Shanghai 200433, China.

[#] These authors contributed equally to this work.

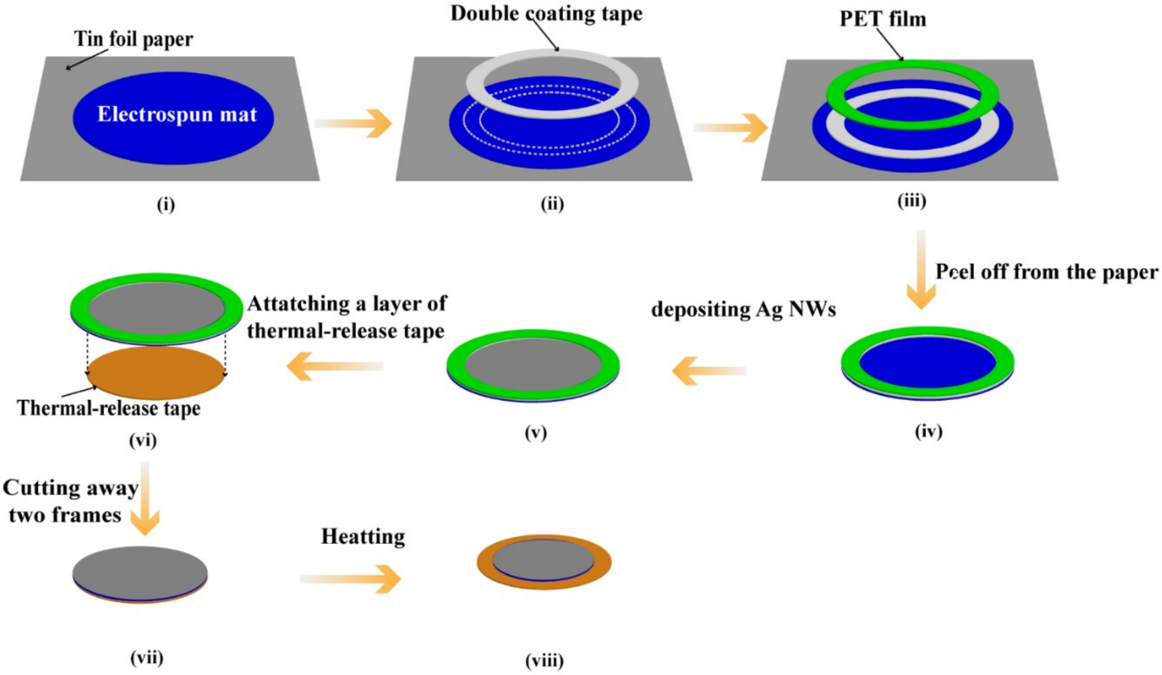

Figure S1. The fabrication schematic of the electrode.

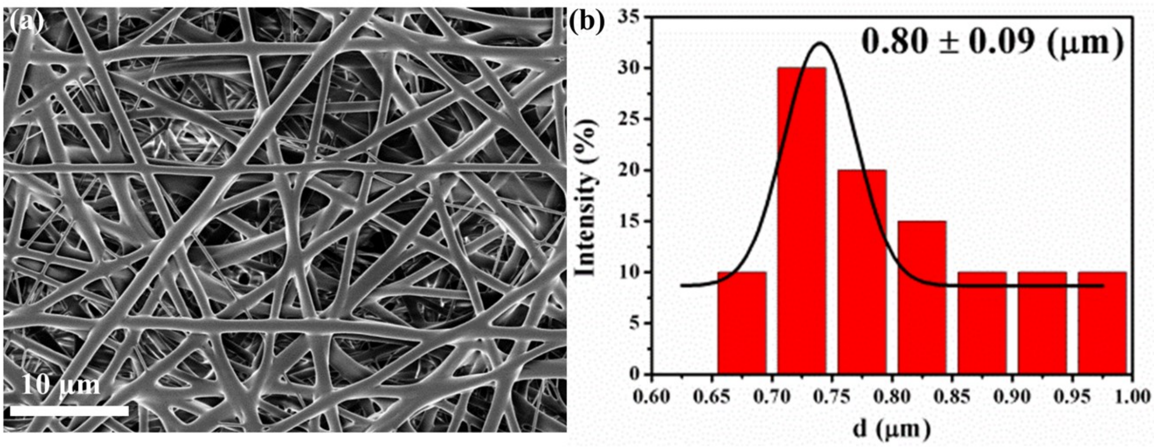

Figure S2. (a) The morphology image of elastic fiber and the diameter distribution of PVDF-HFP microfibers (b).

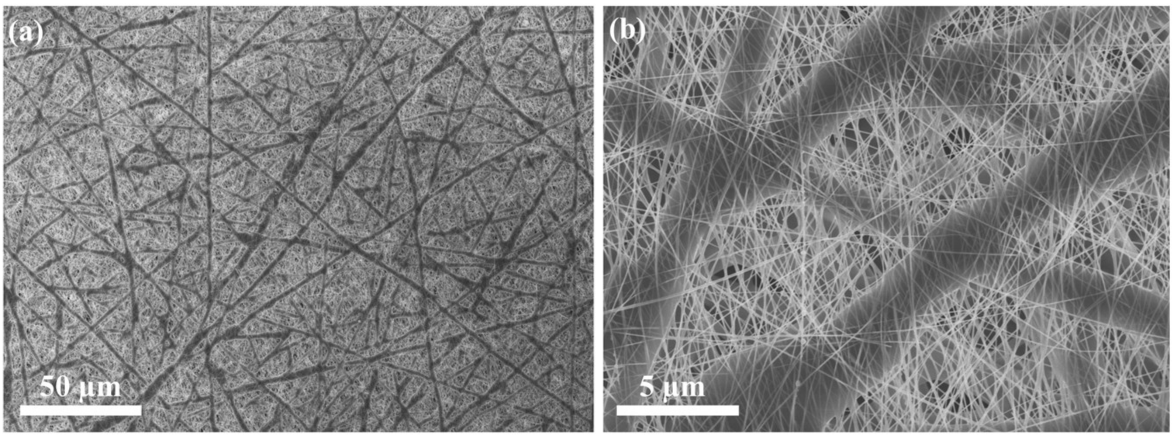

Figure S3. (a) Surface morphology image of polymer mat after depositing Ag NWs (ILQ-15) and its magnified image.

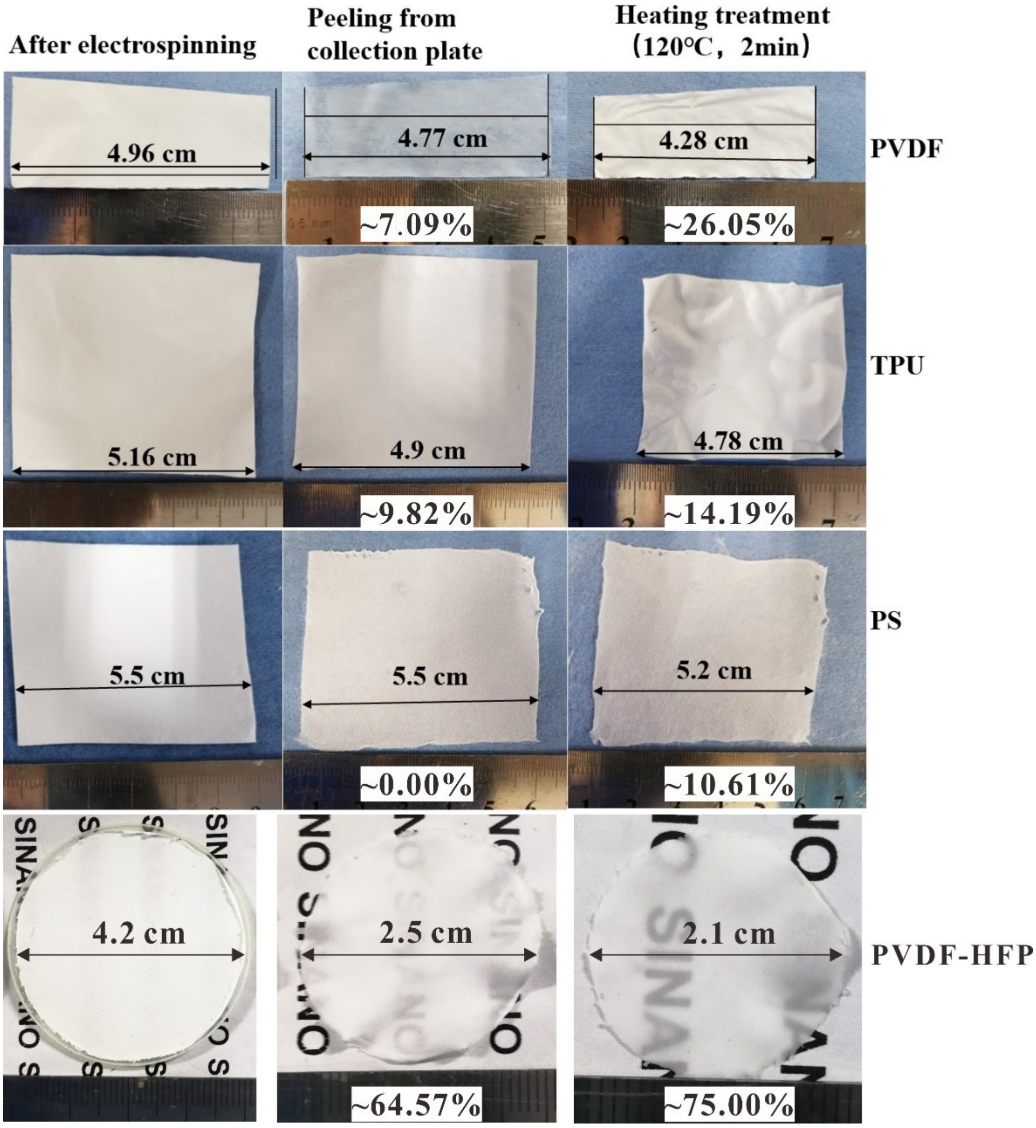

Figure S4. The pictures of electrospun PVDF, PS, TPU, PVDF-HFP fiber mats before and after heat treatment.

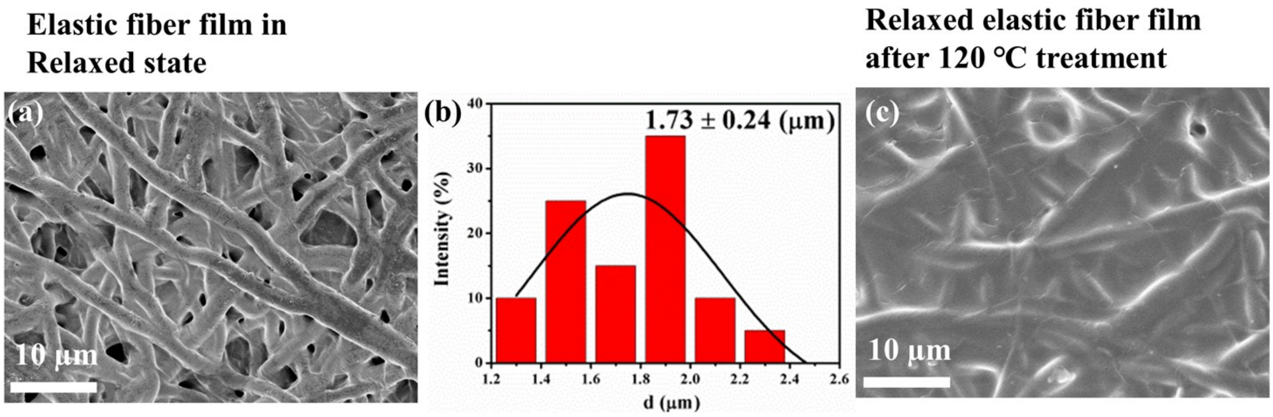

Figure S5. (a) The morphology image of elastic film after being relaxed and the diameter distribution of PVDF-HFP fibers (b), (c) The morphology image of relaxed elastic film after further thermal treatment.

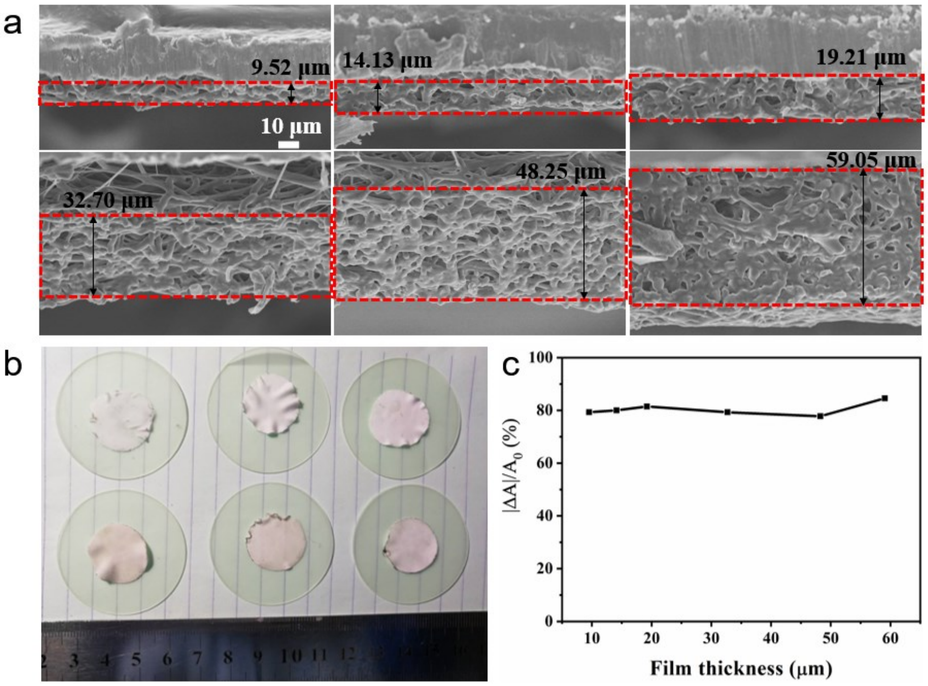

Figure S6. (a) Electrospun fiber mats with different thickness. (b) A digital photo of the fiber mats after heating at 120 °C for 2 min, and (c) their corresponding shrinkage ratios.

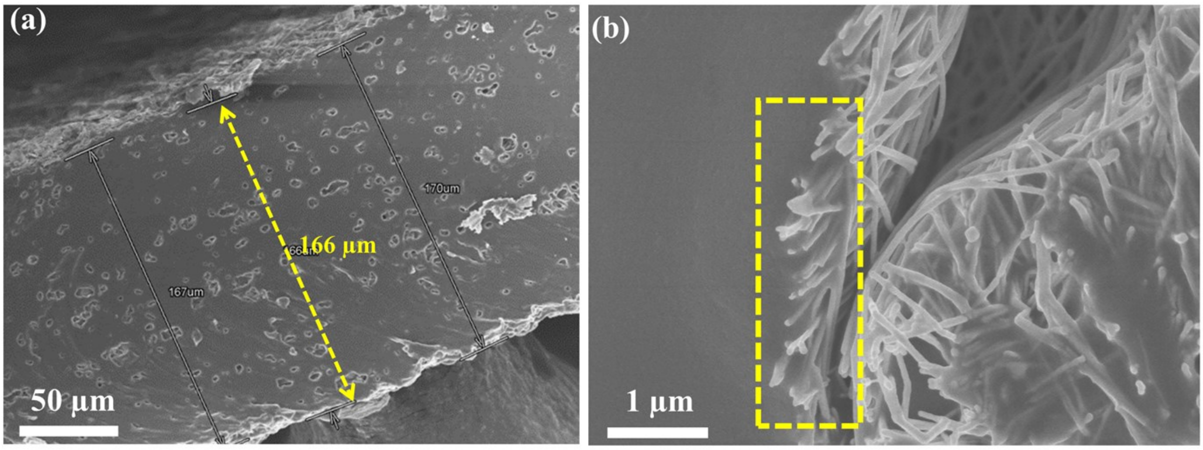

Figure S7. (a) The thickness of a composite electrode, (b) the cross-sectional view of a composite electrode.

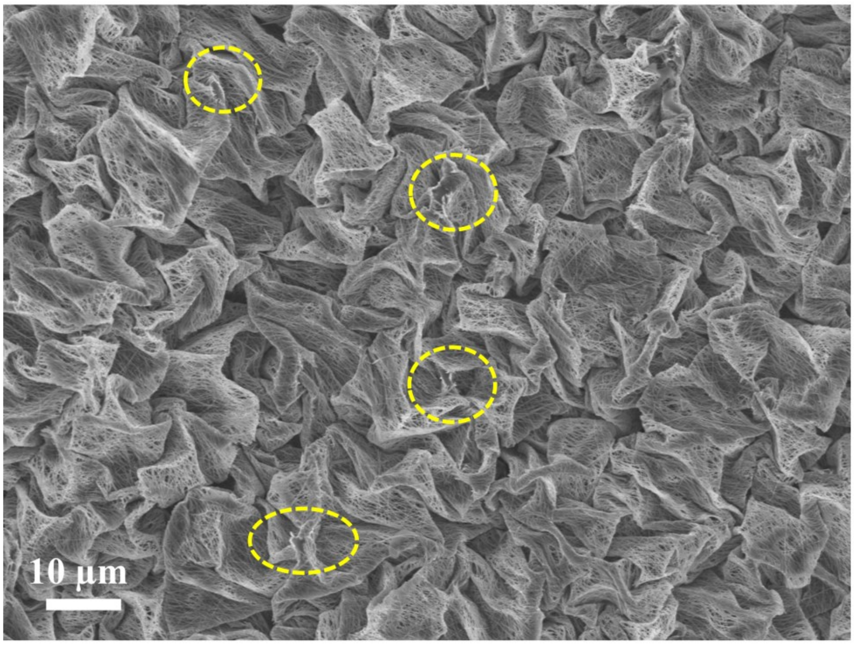

Figure S8. Fractures existing in the conductive layer fabricated using the electrospun mat, V=9 kV, ILQ-30.

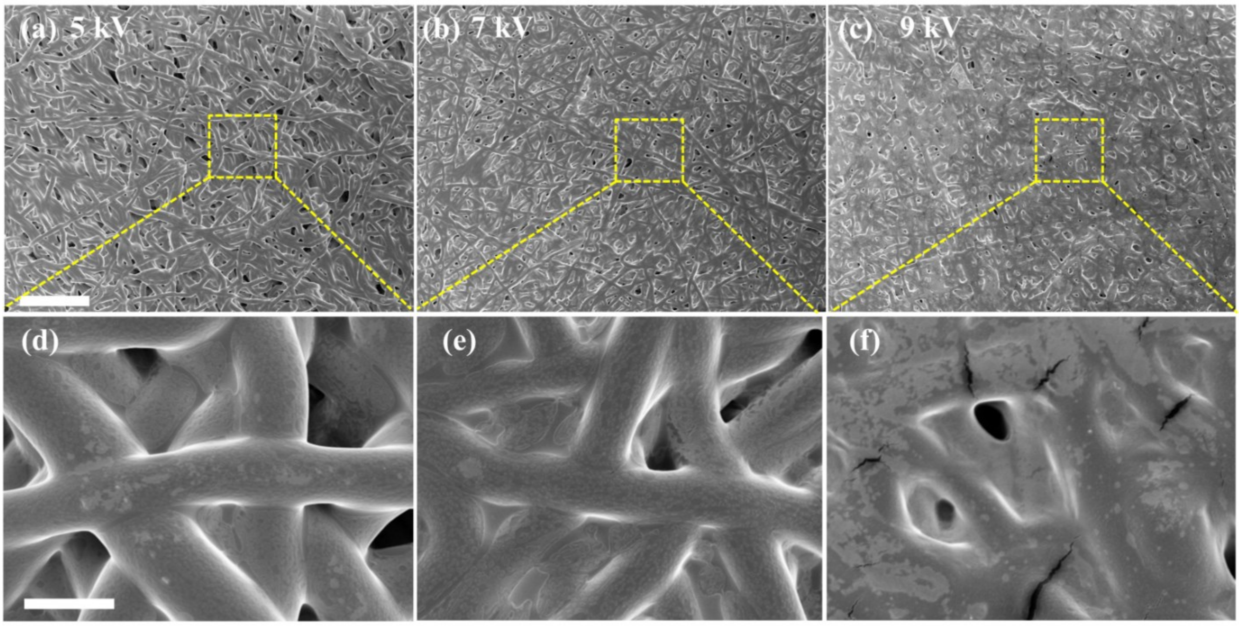

Figure S9. Heated blank film fabricated under different applied voltage. (a)-(c) SEM images of electrospun mats obtained under 5 kV, 7kV and 9 kV, respectively, which had been thermaly treated, as well as their magnified images (d)-(f). The scale bar in (a)-(c) is 50 µm and (d)-(f) is 5 µm.

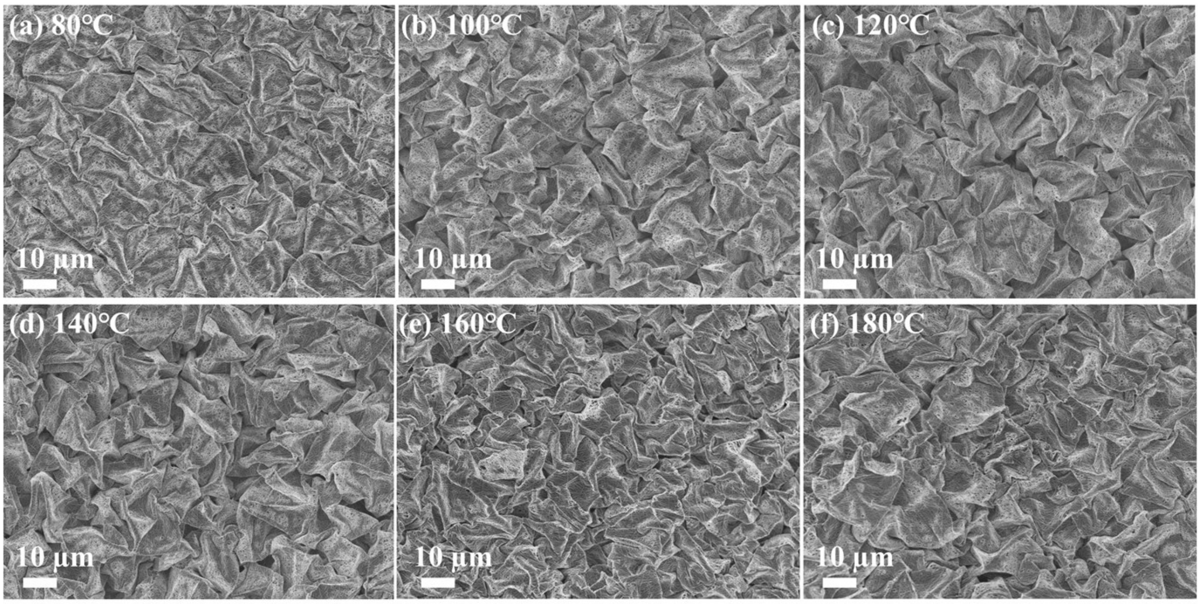

Figure S10. Surface morphology images of electrodes thermally treated at different temperature, 80 °C (a), 100 °C (b), 120 °C (c), 140 °C (d), 160 °C (e), 180 °C (f).

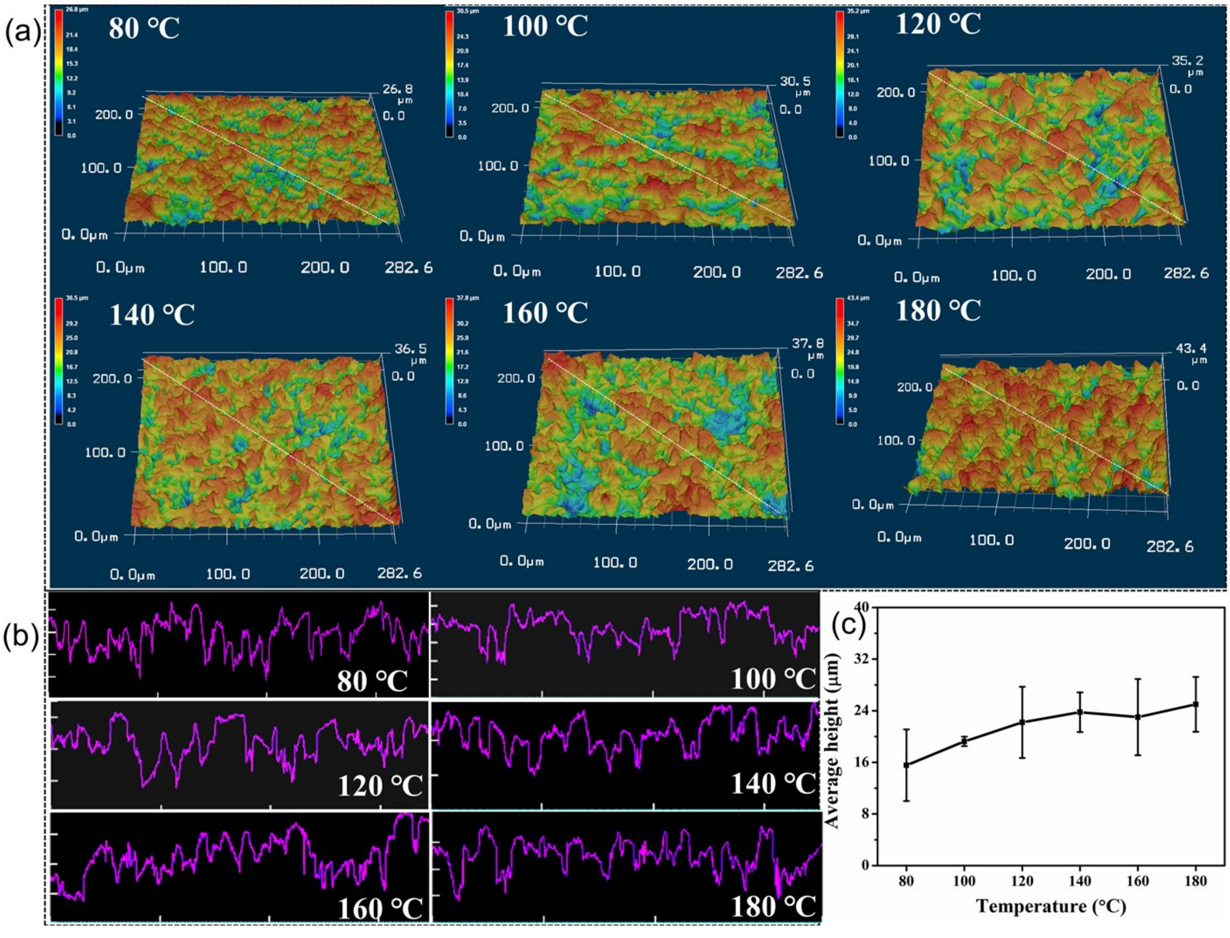

Figure S11. (a) 3D morphology of electrodes fabricated at different temperatures and their profiles measured along the white dashed lines (b) and the relationship between average height versus temperature (c).

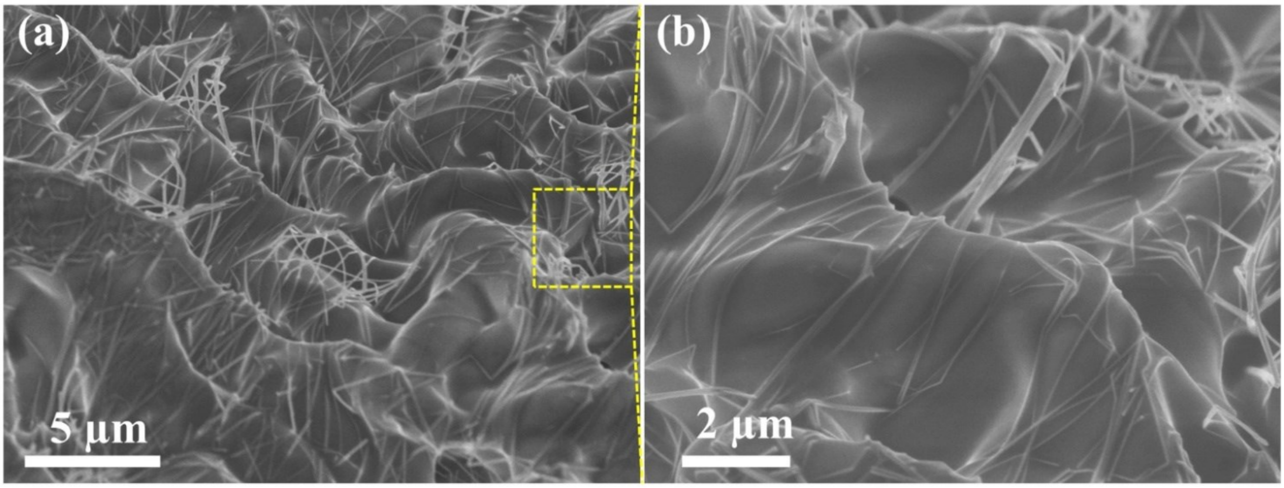

Figure S12. (a) The microscopic morphology of the electrode, ILQ-5 and its magnified image, showning AgNWs embedding into interval of fibers.

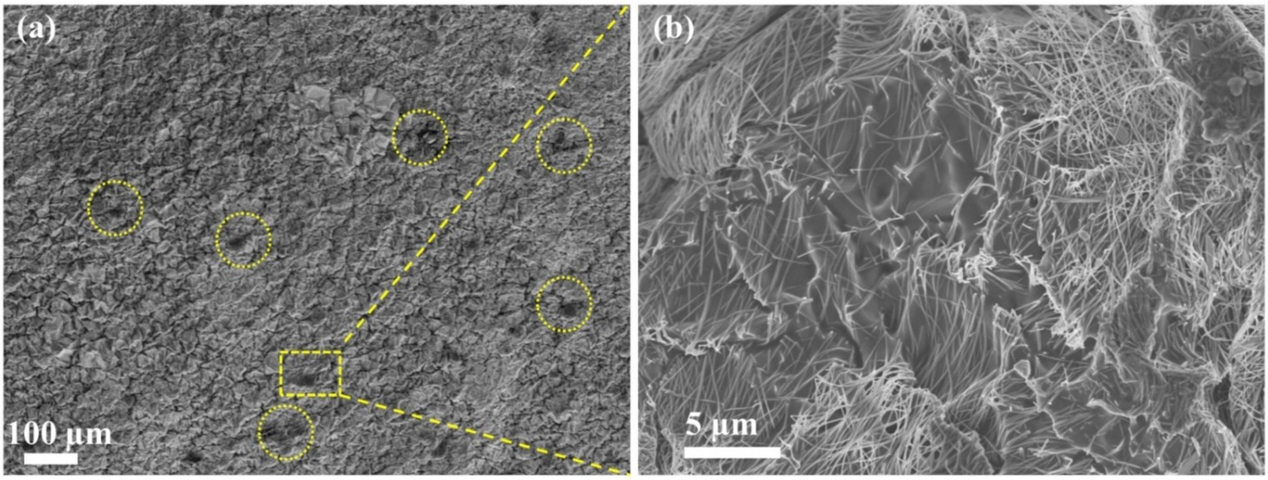

Figure S13. The surface morphology of an electrode after natural releasing.

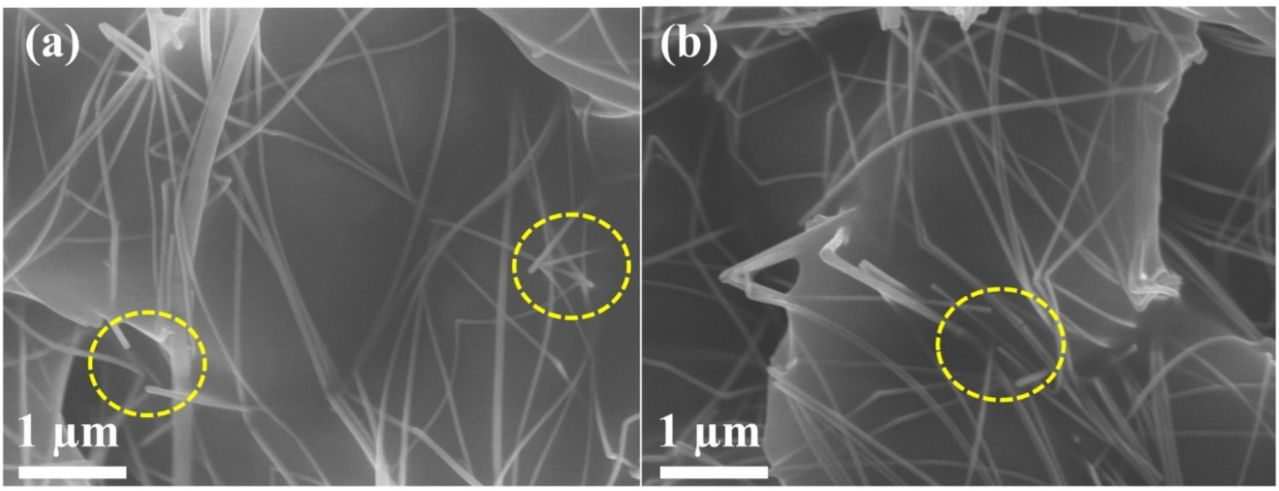

Figure S14. The surface morphology of ILQ-5 (a) and ILQ-10 (b) electrodes after ultrasonic treatment.

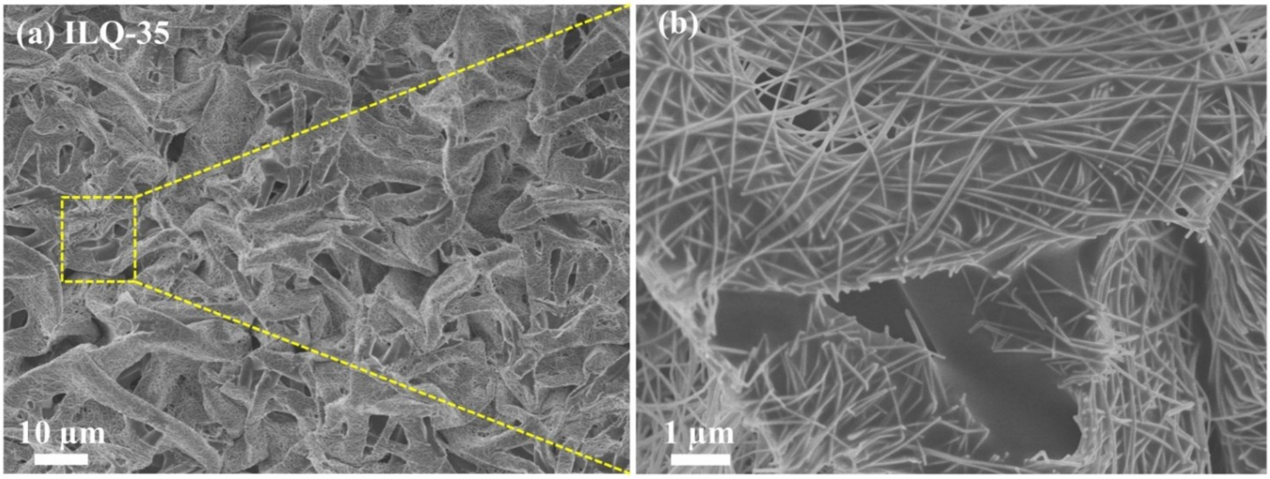

Figure S15. (a) The surface morphology of the electrode (ILQ-35) after ultrasonic and its localised magnified image (b).

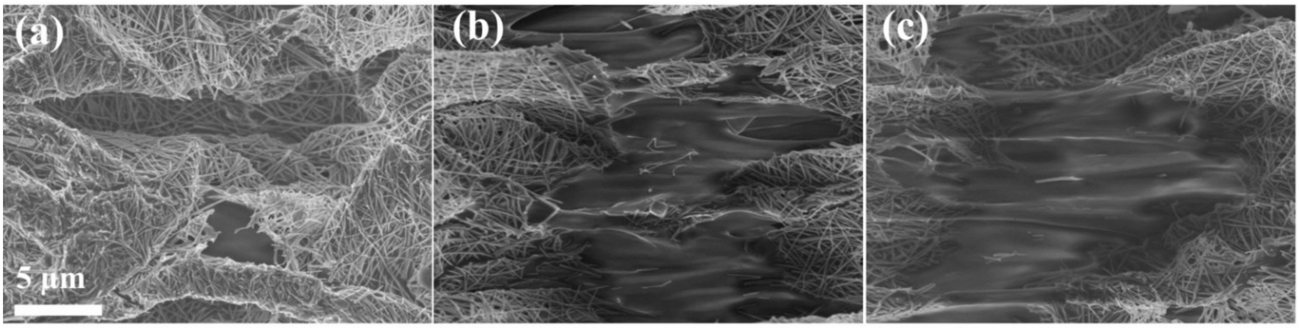

Figure S16. The close-up view of cracks at strain of 200% (a), 300% (b) and 500% (c), corresponding to images in Figure 4 (c).

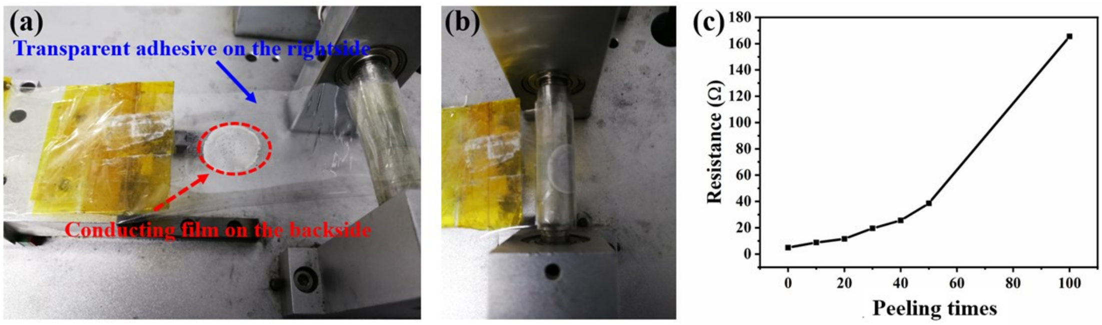

Figure S17. (a, b) The setup for tape test of our electrodes. (c) The resistance changes of electrodes after tape peeling tests.

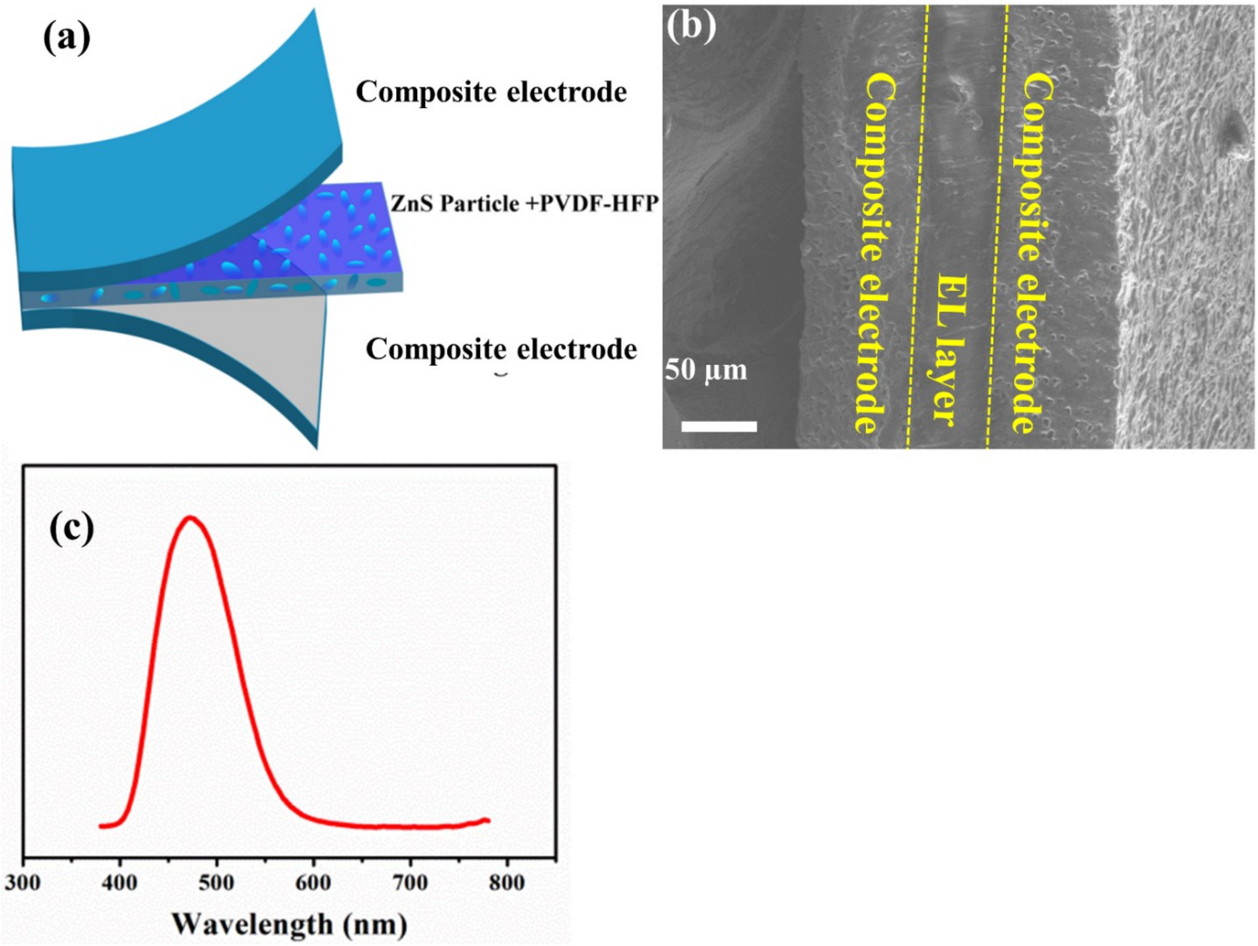

Figure S18. (a) The schematic of EL film, (b) The cross-section image of EL film, (c) The optical spectra of EL film.

Table S1. Performance comparison of the previously reported stretchable electrodes and our electrode.

Method		Materials	Max Stretchability	Electrical performance under strains	Omnidirectional stretchablity	Ref.
Mechanical Pre-stretching	Uniaxial	CNT/PDMS	100%	ΔR/R0=~0.041 at 100% strain	No	1
	Biaxial	MXene/Ag NWs/VHB	100%	$\Delta R_{rct}/R_{0rct}$ =~0.24 at 80% strain	--	2
		Graphene-CNT/rubber	150%	$\Delta R/R_{0rct}$=~2.75 under tensile strain of 150%	$\Delta R_{\square}/R_{0\square}$=0.2 at 140% strain	3
	Multiaxial	rGO nanosheet/PEA	>400%	$\Delta R_{\square}/R_{0\square}$=4 at 400% strain		4
		CNT/PANI	200%	$\Delta R/R_0$=0.025 at 200% strain	$\Delta R/R_0$=0.019 at 80% strain	5
Thermal induced		Au/PDMS	200%	$\Delta R/R_0$=0.3 at 100% strain		6
Solvent swelling and deswelling		Ag film/PDMS	400% in theory	Nearly no change at 100% strain		7
Mold		Ag NWs/ Dragon Skin	150%	$\Delta R/R_0$=6 at 150% strain	No	8
		Graphene/ PDMS	130% in theory	$\Delta R_{\square}/R_{0\square}$=0.67 at 30% strain	$\Delta R/R_0$= ~0.45 under 30% strain, stretched individually along 4 directions	9
3D printing		PEDOT:PSS/ PDMS	270%	Stay constant until breakage	--	10
Electrical field stretching and thermal treatment		Ag NWs/ PVDF-HFP	500%	$\Delta R/R_0$=0.65 at 100% strain	$\Delta R/R_0$= ~1.0 under 80% strain	This work

Note: R_{ct}--charge-transfer resistance

$R_{\square}$---sheet resistance

Reference:

1. F. Xu, X. Wang, Y. Zhu and Y. Zhu, Adv. Funct. Mater., 2012, 22, 1279.
2. T. -H. Chang, T. Zhang, H. Yang, K. Li, Y. Tian, J. Y. Lee and P. -Y. Chen, ACS Nano, 2018, 12, 8048.
3. I. Nam, S. Bae, S. Park, Y. G. Yoo, J. M. Lee, J. W. Han, J. Yi, Nano Energy, 2015 15, 33.
4. J. Mu, C. Hou, G. Wang, X. Wang, Q. Zhang, Y. Li, H. Wang and M. Zhu, Adv. Mater., 2016, 28, 9491.
5. J. Yu, W. Lu, S. Pei, K. Gong, L. Wang, L. Meng, Y. Huang, J. P. Smith, K. S. Booksh, Q. Li, J. -H. Byun, Y. Oh, Y. Yan and T. -W. Chou, ACS Nano, 2016, 10, 5204.
6. J. Kim, S. -J. Park, T. Nguyen, M. Chu, J. D. Pegan and M, Khine, Appl. Phys. Lett., 2016, 108, 061901.
7. N. Gao, X. Zhang, S. Liao, H. Jia and Y. Wang, ACS Macro Lett., 2016, 5, 823.
8. K. -H. Kim, N. -S. Jang, S. -H. Ha, J. H. Cho and J. -M. Kim, Small, 2018, 14, 1704232.
9. J. -Y. Hong, W. Kim, D. Choi, J. Kong and H. S. Park, ACS Nano, 2016, 10, 9446.

10. J. T. Kim, J. Pyo, J. Rho, J. -H.Ahn, J. H. Je and G. Margaritondo, ACS Macro Lett., 2012, 1, 375.